High-frequency losses in tin Josephson tunnel junctions

T. C. Wang* and R. I. Gayley
Department of Physics and Astronomy, State University of New York at Buffalo, Amherst, New York 14260
(Received 20 January 1977)

The losses associated with the excitation of surface plasma oscillations in Fiske modes in tin Josephson junctions, at frequencies from 20 to 270 GHz, were measured by studying the current-voltage characteristics as a function of magnetic field. Our results generally support Economou and Ngai's theory of surface-plasma oscillations and Miller's calculation of the conductivity of superconductors. At lower temperatures, discrepancies that include an anomalous peak in the frequency dependence of the loss may reflect a small disagreement with Miller's results.

INTRODUCTION

There are two types of plasma oscillations that can occur in Josephson tunnel junctions. The first is the Josephson plasma oscillation,[1-3] which involves pair tunneling. It is purely longitudinal; the electric field and current are normal to the insulating barrier, and the magnetic field is zero. The second type is the surface-plasma oscillation (SPO). This is a disturbance running along the surface joining a metal and a dielectric. It involves electromagnetic fields that are localized near the interface and also currents in the metal near the interface. In the case of a tunnel junction, because the dielectric is very thin, the SPO will involve both metal surfaces. It has both transverse and longitudinal character. The electric field and the current density have components normal to and parallel to the tunneling barrier. The magnetic field is parallel to the barrier.

This paper deals with the energy losses associated with SPO in Josephson tunnel junctions. It represents one of the first experimental studies[4,5] of Economou and Ngai's theory of SPO.[6,7] It also provides new support for Miller's calculation of the conductivity of superconductors.[8]

We have determined the energy losses by measuring the quality factor Q of the Fiske modes[9] which appear in a junction's current-voltage characteristic in the presence of a dc magnetic field. When a Fiske mode is excited, the junction is acting as a resonant cavity for an SPO. (In most previous discussions of Fiske modes, reference was made to an electromagnetic wave or to a Swihart[10] wave traveling along the junction. The SPO picture of Economou and Ngai is not really different, but it provides a more detailed physical description.) The coupling between the SPO and the ac Josephson current gives rise to an extra dc current, which we will refer to as a current step, appearing at the voltages corresponding to resonance. By measuring the magnetic field dependence of this extra current, and using a theory due to Kulik,[11] we are able to determine the Q's of the resonances.

Up to now, there have been few measurements of these Q's. Schwidtal and Smiley[12] determined some Q values for Fiske modes in niobium-lead and in lead-lead junctions. While it was not really clear what loss mechanisms were dominant, they argued that at $T/T_c \cong 0.2$ the Q of the niobium-lead junctions was probably determined by the surface resistance of the niobium film, while the Q for the lead-lead case seemed to be limited by nonuniformities in the junction dimensions. Hoffman[4] studied Fiske modes in tin junctions and made the first attempt to compare the measured losses with predictions based on Ngai's[7] and Miller's[8] work. He found agreement for some junctions at $T/T_c \cong 0.5$. Although his accuracy was not great, his results support the idea that the losses are due to surface resistance.

In our laboratory, Gou and Gayley,[13] using techniques similar to those used in the present work, measured Q's for Fiske modes in tin junctions. Because of the small size of their specimens, only a few frequencies could be examined, and the origin of the losses was not clear.

In addition to these Fiske mode studies, there is other work on high-frequency losses which is relevant. Soerensen *et al.*[14] used photon-assisted quasiparticle tunneling to study high-frequency losses in tin junctions. The losses in such a case are very likely to be similar to those occuring in Fiske modes. They concluded that at 35 GHz, the only frequency at which their data gave a clear result, the temperature-dependent losses were due to surface resistance. Finnegan *et al.*[15] concluded that for their lead junctions, which had been designed to maximize radiation, radiation losses made a significant contribution to Q for frequencies from 2 to 12 GHz. Finally, Pedersen *et al.*[3] concluded that the Q of 9-GHz Josephson plas-

ma oscillations in lead junctions is dominated by dissipation due to quasiparticle tunneling. However, it is not clear how this last result is related to SPO losses.

In summary, we can see that the nature of the losses was not really clear, but there was evidence that at least at some temperatures surface resistance is the main contributor.

THEORY

We will take the junction barrier to be a rectangle of length L in the z direction and width W in the y direction. The tunnel current will be in the x direction, and the applied magnetic field will be in the y direction. Then ϕ, the superconducting phase difference across the barrier, has only z and t dependence, and is governed by the following equation[11] (in Gaussian units):

$$\frac{\partial^2\phi}{\partial z^2}-\frac{1}{\bar{c}^2}\left(\frac{\partial^2\phi}{\partial t^2}+\gamma\frac{\partial\phi}{\partial t}\right)=\frac{1}{\lambda_J^2}\sin\phi \quad . \tag{1}$$

Here $\bar{c}\cong c(d_i/\epsilon_i d)^{1/2}$ is the phase velocity of the SPO, for the low frequencies which are of interest to us, ϵ_i is the dielectric constant and d_i the thickness of the insulator, $d=2\lambda+d_i$, λ is the superconducting penetration depth of the metal films, $\lambda_J=(\hbar c^2/8\pi e d j_0)^{1/2}$ is the Josephson penetration depth, j_0 is the maximum Josephson tunnel current density, c is the speed of light, and γ, the damping constant, is related to Q by $Q=\omega/\gamma$, where ω is the angular frequency.

For Fiske modes, we need the solution of Eq. (1) for the case of constant applied voltage and magnetic field. The most detailed solution is due to Kulik,[11] and we will use his analysis to determine Q. A review of this theory and a discussion of how to use it to determine Q from measurements of the temperature and field dependence of the Fiske modes can be found in Ref. 13.

In Kulik's treatment, γ was just a parameter, and Swihart's[10] expression for $\bar{c}$ was used. More recently, in companion papers, Economou[6] and Ngai[7] used the microscopic theory of superconductivity to extend Swihart's analysis to the SPO picture. Of particular interest to us is the fact that Ngai was able to obtain an explicit expression for the Q of the SPO standing waves, assuming a short quasiparticle mean free path in the metal films,

$$Q=2\frac{\sigma_2}{\sigma_1}\left(\frac{\omega}{\bar{c}\,k}\right)^2\Bigg/\left(1-\frac{\epsilon_i\bar{c}^2}{c^2}\right)\times\left(1+\frac{2d_m}{\lambda\sinh(2d_m/\lambda)}\right) \quad . \tag{2}$$

Here $k=2edH_{\text{appl}}/\hbar c$ is the wave number of the Josephson current-density wave when the applied field is H_{appl}, d_m is the thickness of each metal film, and σ_1 and σ_2 are the real and imaginary parts, respectively, of the conductivity of the superconducting metal. Equation (2) gives the Q associated with losses due to quasiparticle currents in the metal, since these are the only losses included in Ngai's analysis. The frequency ω is related to the junction voltage V by the Josephson relation $\omega=2eV/\hbar$. The Fiske mode resonances occur when $\omega=\bar{c}\,k$. For our specimens, d_m is about 140 nm, λ is roughly 50 nm, and d_i is about 2 nm, so that $2d_m/\lambda\sinh(2d_m/\lambda)$ is only 0.02 and $\epsilon_i\bar{c}^2/c^2$ is 0.02. Thus, at the Fiske mode voltages Eq. (2) reduces to

$$Q\cong 2\sigma_2/\sigma_1 \quad . \tag{3}$$

It is interesting to note that Eq. (3) does not contain the geometrical factor that we are accustomed to seeing in expressions for the Q of a cavity. This is because we are dealing with an open ended cavity, and the surface-to-volume ratio is independent of junction length and width.

In order to understand Eq. (3) better and to include other losses, we will discuss the junction cavity in terms of the transmission line equivalent circuit[14,16] shown in Fig. 1. In the figure g_d and g_q are the shunt conductances per unit length due to displacement current in the dielectric and to quasiparticle tunneling, respectively, $r_s=2R_s/W$ is the surface resistance per unit length of the two superconducting films, R_s is the real part of the surface impedance of the superconductor, $l_j=4\pi d/Wc^2$ is the inductance per unit length, $c_j=\epsilon_i W/4\pi d_i$ is the capacitance per unit length, and the symbol J represents the lossless Josephson supercurrent. The diagram does not include the impedance of our current source, which is very large and which will not contribute significantly to the losses. The transmission line is terminated at each end by an output impedance $Z_0=(\mu_0/\epsilon_0)^{1/2}$.

We can determine a Q value for each type of loss by supposing that each is the only one present. For the

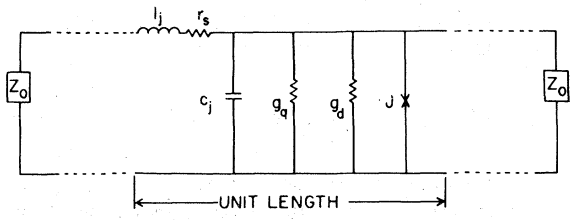

FIG. 1. Transmission line equivalent circuit of a Josephson tunnel junction. The quantities l_j, c_j, r_s, g_q, and g_d are the inductance, capacitance, surface resistance, quasiparticle tunneling conductance, and displacement current conductance, per unit length, respectively. The lossless Josephson tunnel current is represented by J, and Z_0 is the output impedance.

quasiparticle currents, which give rise to the surface resistance, we see a simple RLC circuit, for which Q is $\omega l_j/r_s$. Dielectric losses give a Q of $\omega c_j/g_d$, and for quasiparticle tunneling the relation is $\omega c_j/g_q$. The Q due to radiation from the ends of the junction is given by the familiar relation

$$(Z_j+Z_0)^2/4Z_jZ_0 \ ,$$

where

$$Z_j=[(r_s+j\omega l_j)/(g_d+g_q+j\omega c_j)]^{1/2} \ ,$$

and the factor $j=(-1)^{1/2}$.

Another contribution to Q arises from variations in the junction length. Sections of different length will have different resonant frequencies, so that the resonance is broadened in frequency. We will refer to this as the geometric effect. If the variation in length is ΔL, the corresponding Q will be $L/\Delta L$.

The net Q is determined by adding the reciprocals of the various contributions. Thus,

$$\frac{1}{Q}=\frac{1}{Q_s}+\frac{1}{Q_d}+\frac{1}{Q_q}+\frac{1}{Q_r}+\frac{1}{Q_g} \ , \tag{4}$$

where the subscripts s, d, q, r, and g denote surface resistance, dielectric, quasiparticle tunneling, radiation, and geometrical, respectively.

We will see that in our specimens, at least at higher temperatures, Q_s gives the principle contribution to Q, so that Eq. (3) should give the net Q. It is interesting that we can give a simple derivation of that equation using the equivalent circuit picture. First, X_s, the imaginary part of the surface impedance of a metal film, is given by[17] $X_s=4\pi\omega\lambda/c^2\cong 2\pi\omega d/c^2$, where we have used the fact that d is approximately 2λ. Then the inductance per unit length $l_j=2X_s/\omega W$. Since $r_s=2R_s/W$, we obtain

$$Q_s=\omega l_j/r_s=X_s/R_s \ . \tag{5}$$

Second, we will suppose that the quasiparticles behave like normal electrons and use the theory of surface resistance developed for normal metals.[18] Ngai assumed that the quasiparticle mean free path l is much smaller than the electromagnetic penetration depth, in which case the surface impedance Z is

$$Z=R_s+jX_s=(2\pi\omega/c^2\sigma)^{1/2}(1+j) \ , \tag{6}$$

where σ is the complex conductivity $\sigma(\omega)=\sigma_1(\omega)+j\sigma_2(\omega)$. In the frequency range of interest, σ_1 is much less than σ_2, so that Eqs. (5) and (6) reduce to Eq. (3). This is Ngai's[7] result, for the thick film case. The success of our simple derivation implies that this particular result of Ngai is not sensitive to the details of his model. [Of course, Eq. (2) does contain those details. This relation could be tested by using smaller values of d_m/λ, but we have not attempted this.]

Our specimens do not really satisfy the short-l assumption used in deriving Eq. (3). We found the mean free path of a typical film to be 92 nm by measuring its residual resistivity ratio. The coherence length for pure tin is about 300 nm, and, according to Miller's calculations,[8] the penetration depth in the metal films is close to 60 nm for all the frequencies and temperatures studied in the present work. Thus, all of these characteristic lengths are of the same order of magnitude. Our specimens do not correspond to either of the simple limiting cases: the local limit and the extreme anomalous limit. Waldram[19] has presented evidence that the real part of the superconducting surface impedance is not a strong function of l. However, except very near T_c, a temperature range that is not relevant to our measurements, he was not able to give any simple results for the imaginary part. In the absence of any better guidance as to the expected surface resistance, we will try both limiting cases. For the local limit, this means using Eq. (3) and Miller's[8] calculated values of σ_1/σ_n and σ_2/σ_n, where σ_n is the normal state conductivity. For the other limit, we will actually use a modification of the extreme anomalous limit. We start with Miller's expression[8]

$$Z_{\infty,s}/Z_{\infty,n}=[(\sigma_1-j\sigma_2)/\sigma_n]^{-1/3} \tag{7}$$

for the ratio of superconducting to normal surface impedance in the extreme anomalous limit. Miller pointed out that even in pure tin this limit is not achieved because the coherence length is not long compared to the penetration depth. To get a better approximation, he assumed $l=\infty$ but took the correct coherence length and numerically computed r/r_∞ and x/x_∞. The subscript refers to the extreme anomalous limit (l and coherence length both infinite), $r=R_s/R_n$, and $x=X_s/X_n$. Equations (5) and (7) give

$$Q_\infty=X_{\infty,s}/R_{\infty,s}=3\sigma_2/\sigma_1 \ , \tag{8}$$

and Q_∞ is computed from Miller's values of σ_1/σ_n and σ_2/σ_n. The modified extreme anomalous limit is then obtained by correcting Eq. (8) by the factors r/r_∞ and x/x_∞, giving

$$Q=Q_\infty(x/x_\infty)/(r/r_\infty) \ . \tag{9}$$

RESULTS AND DISCUSSION

High-quality in-line tin Josephson tunnel junctions were made by the technique developed by Paley *et al.*[20] and also used by Gou and Gayley.[13] Briefly, the tin films were deposited on a cooled sapphire substrate at a pressure below 2×10^{-6} Torr. The oxide was grown immediately after the first film was deposited, using an oxygen glow discharge method. The vacuum was then broken to change the deposition mask, and

TABLE I. Specimens. Temperature-dependent quantities were evaluated at $T/T_c = 0.36$. The gap frequency is related to the energy-gap voltage $2\Delta/e$ by the conversion factor 484 GHz/mV.

Specimen No.	Transition temperature T_c (K)	Gap frequency (GHz)	Frequency of $n=1$ Fiske mode (GHz)	Josephson current density j_o (A/cm^2)	Film thickness d_m (μm)	Length L (mm)	Width W (mm)	L/λ_J
N18	3.73	524	27	7.24	0.12	0.32	0.17	1.68
N20	3.73	520	24	0.73	0.14	0.36	0.21	0.60
N26	3.76	532	47	13.93	0.14	0.19	0.20	1.41
N27	3.76	532	32	0.74	0.15	0.24	0.14	0.41
N28	3.76	540	35	13.38	0.13	0.23	0.12	1.66

then the second tin film was laid down.

The techniques used for studying the Fiske modes of these specimens were the same as those reported by Gou and Gayley, except that the measurements were carried out in a shielded room.

Table I lists the properties of our specimens. The dimensions L and W were measured in a microscope, d_m was determined with an interferometer, and the other quantities were determined from the junction current-voltage characteristic.

Figure 2 shows an example of the magnetic field dependence of Fiske mode current step heights. In the figure, I_n is the step height of the nth mode, averaged from the four values obtained from reversing the applied field and measuring current directions, and I_0 is the maximum zero-field zero-voltage supercurrent. The solid lines were computed using Kulik's theory, in which H_0 is the field which produces one flux quantum in the junction. In computing these curves, Q and H_0 were chosen so that experiment and theory coincided at the maximum step height for any mode I_n^m. Thus, our Q values were determined from the I_n^m. Note that each curve is a two parameter fit, and H_0 is different for each. (In Ref. 13, only Q was adjusted; H_0 was determined from the field dependence of the zero-voltage supercurrent. As a result, Fig. 2 shows a somewhat better fit than does Fig. 3 in Ref. 13.) If we regard the H_0 determined from the zero-voltage supercurrent as the true value, then the H_0's used in Fig. 2 were shifted by varying amounts of 10% or less. Such small changes in H_0 have a negligible influence on the value determined for Q.

The agreement with theory is reasonably good, especially since some of our specimens do not really satisfy the assumption of Kulik's theory that $(L/\pi n \lambda_J)^2$ is very much less than one.[21] (L/λ_J values are given in Table I.) This gives further support to Gou and Gayley's inference that Kulik's theory can be used to determine Q values from our data.

One specimen, No. N28, does show some significant discrepancies with the theory. The most serious occurs for the $n=1$ mode at our lowest temperature, $t \equiv T/T_c = 0.36$. The field dependence of I_1 shows two closely spaced peaks instead of the single broad peak predicted. In this case, we do not know how to determine Q, since Kulik's theory is not followed. We elected to determine Q from the peak which was right at the correct field, for lack of any better method. We will discuss this anomalous specimen later.

As shown in Fig. 2, the mode step height I_n is a function of applied field and has a maximum value I_n^m. One of the important features of Kulik's theory is that, as the temperature decreases below the superconducting transition temperature T_c and Q increases, I_n^m increases to a maximum value and then decreases. We call the maximum value $(I_n^m)^m$. Figure 3 shows examples of the temperature dependence of I_n^m. Maxima occur for $n=1$, 2, and 3. Presumably, $n=4$ would also show one, if Q could be made large enough. The

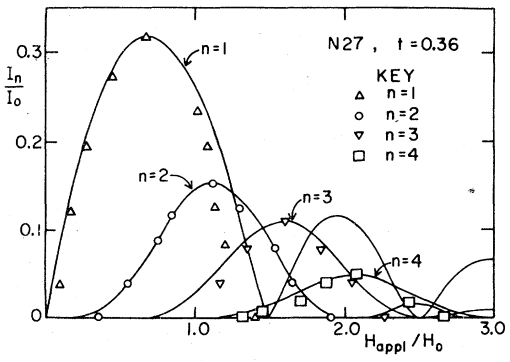

FIG. 2. Typical magnetic field dependence of Fiske modes. I_n is the current step height for the nth mode, and I_0 is the maximum zero-voltage supercurrent in zero field, at the same temperature. H_{appl} is the applied field, and H_0 is nominally the field that will produce one quantum of flux in the junction. The solid lines were computed from Kulik's theory, with Q and H_0 chosen for each n so as to make theory and experiment agree at the maximum value of I_n.

existence of such maxima was first clearly demonstrated in Ref. 13. However, because of the different junction parameters used in that work, it could only be shown clearly for $n=1$. Now we see that I_n^m decreases at low temperatures for other modes as well. As in Ref. 13, we usually find the value of $(I_n^m)^m$ to be in good agreement with theory.

However, the experimental values of $(I_n^m)^m$ are not exactly as predicted. For example, for specimen *N*26, $(I_1^m)^m/I_0$ was 0.38, instead of the theoretical value of 0.37, and $(I_2^m)^m/I_0$ was 0.34, a little smaller than the predicted 0.35. These discrepancies, though small, require some adjustment of our results. When any observed I_n^m exceeds the theoretical value, the theory gives no answer for Q. On the other hand, when $(I_n^m)^m$ is below the predicted value, an unphysical discontinuity in Q versus T will result from a straightforward application of the theory. For the examples cited, the problem is obviously quite minor, so we adopted the simple device of adjusting the I_0 value used for each mode so that $(I_n^m)^m$ would have the theoretical value. Except for specimen *N*28, the resulting changes in Q were less than 20% and do not affect our general conclusions. One mode, $n=3$ for specimen *N*28, is the exception. Theory gives $(I_3^m)/I_0=0.34$, while the observed value was only 0.18. We adjusted I_0 in this case also, but obviously we cannot have confidence in the resulting Q.

We have seen two respects in which *N*28 was anomalous. $(I_3^m)^m$ had only about half the expected value, and the field dependence of I_1 at $t=0.36$ was peculiar. The resulting Q values are highly questionable, and we feel that all of the results for this specimen must be viewed with suspicion, even though in all other respects this junction was quite conventional. For this reason, the Q values for *N*28 will be presented separately.

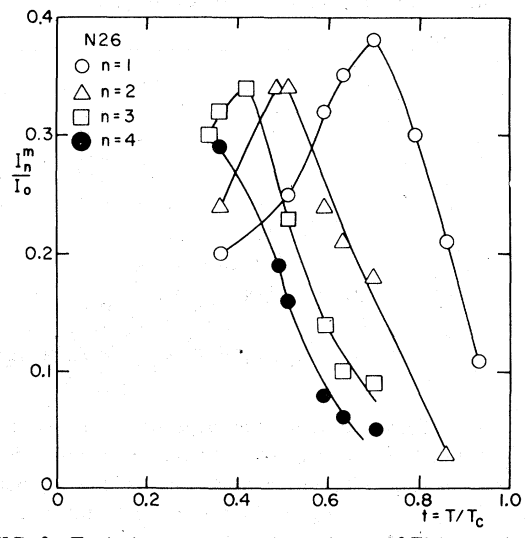

FIG. 3. Typical temperature dependence of Fiske modes, showing that the step height passes through a maximum as the temperature is lowered. I_n^m is the maximum value of the step height I_n at whatever field maximizes it.

Figure 4(a) shows our results for all of the specimens of Table I except *N*28. We also have not included any data from Ref. 13. The reason for excluding results from Ref. 13 stems from the fact that the latter work dealt with smaller specimens. This would give a smaller geometrical Q, Q_g, which is consistent with the fact that those specimens tended to have lower Q's, particularly at the lower temperatures. Since those specimens have been destroyed, there is no way to check their variation in length, but assuming that they had ΔL values comparable to those measured on the present junctions easily accounts for any differences between those results and the present ones. Lacking knowledge of ΔL, we have omitted the data from Ref. 13 in our analysis.

Figure 4(a) therefore summarizes the behavior of four junctions at four different temperatures. The temperatures were selected as the ones for which Miller[8] had calculated σ_1 and σ_2. The horizontal axis is $\hbar\omega/\Delta(T)$, where $\Delta(T)$ is the half-gap, in energy units, at the temperature in question. For a given specimen, different ω values correspond to different modes. For example, for *N*26 at $t=0.36$, there are eight points, corresponding to the $n=1-8$ modes that were observed. All of the data ends near $\hbar\omega/\Delta=2$, which corresponds to a mode lying at a voltage of half the energy-gap voltage. As the frequency increases through this vicinity, losses increase rapidly due to pair breaking, and the modes become unobservable. However, it was not always possible to find modes even this far out. For *N*27, for example, the largest n observed at $t=0.36$ was 6, at $\hbar\omega/\Delta=1.38$. At $t=0.63$ the largest value was $n=4$, at $\hbar\omega/\Delta=1.12$. We do not know why there is this variation in highest observed $\hbar\omega/\Delta$. However, we do know that noise can be very troublesome. An increase in noise level can cause a small current step to disappear completely. Thus it is easy to imagine that variations in the cutoff value of $\hbar\omega/\Delta$ are due to variations in the relative severity of noise.

All in all, these specimens agree with each other quite well. The experimental uncertainty, indicated by error bars on some of the points, is comparable to the spread of the data, except for the point for specimen *N*27, $\hbar\omega/\Delta=1.38$, $t=0.36$. This case has $Q^{-1}=1.5\times10^{-2}$, whereas according to the other specimens it should be more like 0.9×10^{-2}. The solid lines were drawn by eye to suggest the average behavior of the specimens. We take these lines to be our result for the frequency and temperature dependence of Q^{-1} in our junctions.

These lines are reproduced in Fig. 4(b), along with the data for junction *N*28. As mentioned previously,

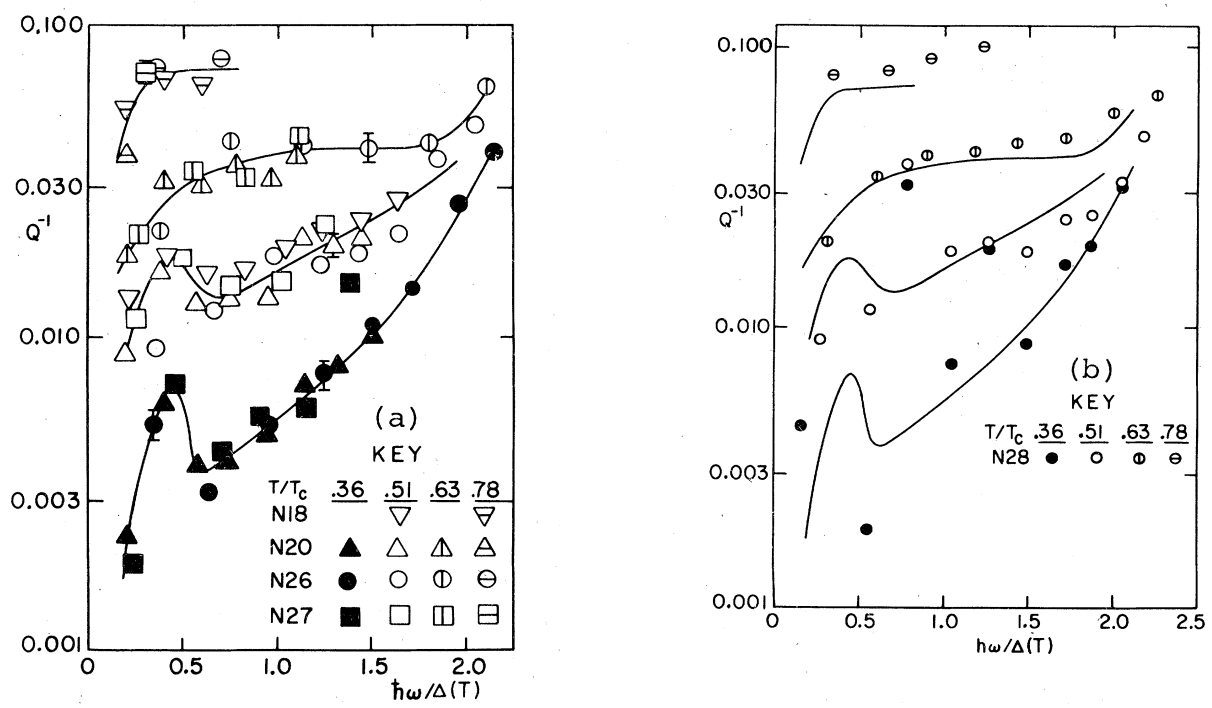

FIG. 4. Temperature and frequency dependence of the reciprocal of the quality factor Q for Fiske modes in tin junctions. The frequency ω is determined from the voltage of each mode, and $2\Delta(T)$ is the energy gap at the temperature of the measurement. The reduced temperatures $t = T/T_c$ are indicated. (a) Results for specimens $N18$, $N20$, $N26$, and $N27$. The solid lines were drawn by eye, to suggest the average behavior of these specimens; (b) results for $N28$. These are presented separately since, as explained in the text, we do not have confidence in the results obtained with this specimen. The solid lines were copied from (a).

all of the $n=3$ ($\hbar\omega/\Delta \cong 0.8$) Q values are highly suspect, as is the $n=1$, $t=0.36$ value. Consider first the $n=3$ case. At $t=0.78$ and 0.63, it lies close to the curve obtained from the other specimens. At lower temperatures, Q^{-1} appears to change little, but it must be emphasized that this may be an artifact of the method used to compute Q. The other questionable Q value, for $n=1$ at $t=0.36$, lies quite close to the experimental curve. Most of the other points are also close to the curves, but the $t=0.36$, $n=2$ ($\hbar\omega/\Delta=0.55$) and $n=5$ ($\hbar\omega/\Delta=1.26$) points, which were not expected to be anomalous, are quite far off. We do not know what to make of these discrepancies. By the usual criteria, $N28$ is a very good specimen. Its zero-voltage supercurrent versus field "interference curve" is good, as is its current-voltage characteristic and maximum supercurrent. It does have a rather large value of L/λ_J, but then so do $N18$ and $N26$. Our justification for excluding $N28$ then lies in that (i) some of the Fiske mode behavior differs greatly from Kulik's theory, and (ii) some of the Q results differ greatly from that of our other specimens. However, we have no basis for regarding the specimen as defective, so the data have been presented here for completeness.

The curves from Fig. 4(a) have also been reproduced as solid lines in Fig. 5, along with the theoretical curves. The dashed lines show the local limit, Eq. (3). The dotted lines, shown at two temperatures only, are for the modified extreme anomalous limit, Eq. (9). There are no adjustable parameters in this figure, and the agreement between experiment and the local limit, at the higher temperatures, seems quite impressive. For example, at $t=0.63$ both the magnitude and the frequency dependence are quite close. On the other hand, the modified extreme anomalous limit prediction for Q^{-1} at that temperature is too large by 50% or more.

Our interpretation of Fig. 5 is that the agreement at higher temperatures shows that the local limit formula

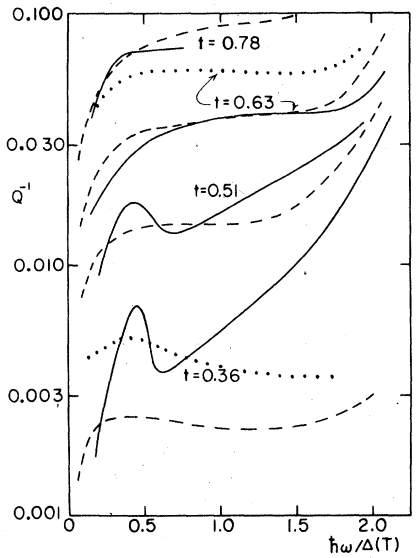

FIG. 5. Comparison between theory and experiment. The solid lines, copied from Fig. 4(a), represent our experimental results. The dashed lines were computed from Ngai's formula $Q=2\sigma_2/\sigma_1$ [Eq. (3)], and the dotted lines, shown only at $t=0.63$ and $t=0.36$, and the modified extreme anomalous limit [Eq. (9)].

is adequate for our specimens even though l is not as short as this limit requires. If this is true at $t=0.63$, it should also be true at lower temperatures, since none of the characteristic lengths will change significantly. Therefore, we believe that the difference between experiment and the local limit which is apparent at $t=0.36$ is due to something other than a failure of Eq. (3).

At $t=0.36$ there are two kinds of discrepancy between theory and experiment. First, Q^{-1} is too large, particularly at high frequencies. Second, there is a pronounced bump at $\hbar\omega/\Delta$ near 0.5. This bump also shows clearly at $t=0.51$. Keeping in mind the experimental error indicated in Fig. 4(a), we interpret the deviations between theory and experiment to be in the direction of the experimental Q^{-1} being larger than the theoretical one. This then allows the discrepancies to be attributed to other loss mechanisms. However, there are two other possibilities that should be considered. One is that the bump might be due to some other resonance. The second is that we are seeing some error in the theoretical calculations of σ_1 and σ_2.

Let us first consider the possible role of other loss mechanisms. The radiative contribution to Q^{-1} will be $Q_r^{-1}=4Z_jZ_0/(Z_j+Z_0)^2$. The junction impedance Z_j is approximately $(l_j/c_j)^{1/2}$ for our case. Using the expressions given before, this reduces to $Z_j=(\bar{c}c_j)^{-1}$. For our junctions $\bar{c}=1.4\times10^7$ m/sec and $c_j=5.3\times10^{-6}$ F/m, giving a Z_j of roughly 0.014 Ω and $Q_r^{-1}=0.14\times10^{-3}$. For losses due to quasiparticle tunneling, we have $Q_q^{-1}=g_q/\omega c_j$. From the current-voltage characteristics of our junctions, we can see that g_q is no greater than 58 $(\Omega\text{m})^{-1}$ at $t=0.51$, and it must be even smaller at lower temperatures. Choosing our smallest frequency, 20 GHz, gives $Q_q^{-1}\leq0.6\times10^{-3}$. At higher frequencies and at lower temperatures this figure will be smaller. Dielectric losses are harder to estimate, since little is known about the properties of the oxide in junctions where the oxide thickness is of the order of 2 nm. We expect these losses to be small because most of the volume of the region having ac fields is in the metal, but at a sufficiently low temperature this may cease to be a correct conclusion. Soerensen *et al.*[14] used numbers appropriate to bulk tin oxide to estimate $Q_d^{-1}+Q_q^{-1}<10^{-3}$. This is consistent with our estimate of Q_q^{-1}, and we will use it for lack of anything better. The geometric contribution to Q^{-1} was determined by examining the specimens in a measuring microscope. Typical results were $L\cong0.3$ mm and $\Delta L\cong10^{-3}$ mm, giving $Q_g^{-1}\cong3\times10^{-3}$.

In summary, Q_g^{-1} appears to be the largest contribution to Q^{-1} after Q_s^{-1}. Figure 5 suggests that Q_s^{-1} is the principle contribution and that losses in our junctions are due primarily to the surface resistance of the metal films. According to the above estimates it is possible that the low-frequency modes at $t=0.36$ have a significant broadening due to the geometric effect. This effect will limit Q^{-1} to the order of 10^{-3} or Q to about 1000, unless junctions of improved uniformity are constructed. Even if this is done, other losses will probably prevent Q from rising much above 1000. Finally, it appears that the discrepancies shown in Fig. 5 cannot be attributed to other loss mechanisms.

With respect to the bump in Q^{-1} at $\hbar\omega/\Delta$ near 0.5, which is a frequency of about 60 GHz, none of the known losses have the kind of frequency dependence that could explain it. The shape does make one think of resonant coupling with another resonator, perhaps external to the junction. Note that all the junctions give a bump at the same frequency, rather than at the same n value. Our specimens were mounted in the center of a copper solenoid 1.78 cm in diameter. This diameter corresponds to a cylindrical cavity resonance of roughly 80 GHz. We ruled out the possibility that this was a factor by repeating some of the measurements with a 3.20-cm-diam solenoid. The only other candidate would be the Dewar tail itself. However, it is outside the solenoid, and it is made of brass, which is quite lossy. We do not think that it is likely to contribute.

Another possible interpretation of the bump is that we are seeing another mode of excitation of the junction, so that our Q determinations are completely wrong at this frequency. This seems unlikely since the junction lengths differ by a factor of 2 and yet all

give a bump at the same frequency. In any case, we know of no other mode, including the "additional solutions" mentioned by Kulik,[11] that could be excited under the conditions of our experiment.

Several other points should be made about the bump. First, note that the vertical scale in Fig. 4(a) is logarithmic. Numerically, the size of the bump is roughly the same at $t=0.36$ and $t=0.51$, and a bump of this magnitude would be impossible to detect at higher temperatures. Therefore the height of the bump may be independent of temperature. Second, examination of Fig. 4 will show that a given specimen may show additional bumps at higher frequencies. However, none of these reproduces from specimen to specimen, and they are probably not real. Finally, it is curious that Economou[6] presented a graph of Q^{-1} versus frequency, based on Miller's values of σ_1 and σ_2, which shows an abrupt bump near $\hbar\omega/\Delta=0.5$ at $t=0.51$. It turns out that this was a numerical error, as Economou has confirmed,[22] and the dashed curves of Fig. 5 are the proper ones. However, Fig. 5 shows that Miller's results do give a slight bump at $t=0.36$.

On the basis of the preceding discussion, it seems possible that the discrepancies of Fig. 5 are a real disagreement with Miller's calculation of σ_1 and σ_2. His results have been tested at other frequencies[23–26] and found to be reasonably good. Therefore, we would hesitate to suggest that there are any serious errors. However, our theoretical curves are determined by the ratio of σ_2 and σ_1, so that in fact only modest adjustments in Miller's results would be required to obtain agreement. Considering the approximations involved in the theory, such adjustments seem quite reasonable.

CONCLUSIONS

Our results provide the first experimental test of both the real and imaginary parts of the conductivity of superconducting tin, as calculated by Miller, at frequencies as high as 270 GHz. The agreement is good except at lower temperatures. If, as we suspect, the disagreement at low temperatures is due to a real discrepancy between theory and experiment, our results will be useful in testing improved calculations. The bump which we found in Q^{-1} at 60 GHz will be particularly sensitive to the details of any theoretical result.

Our work indicates that the high-frequency losses associated with the excitation of surface plasma oscillations in tin Josephson tunnel junctions are due to the surface impedance of the tin films, except perhaps at lower temperatures. Our results support the surface plasma oscillation picture of Economou and Ngai, although this support is not particularly strong since it depends only on the formula $Q=2\sigma_2/\sigma_1$.

The bump in Q^{-1} versus frequency is a particularly curious feature of our results. It shows that in a rather narrow frequency range the losses are unusually high. It would be interesting to see if this bump grows larger at lower temperatures, since it might then be easier to deduce its origin.

---

*Present address: Dept. of Physics, State University of New York at Stony Brook, Stony Brook, N.Y. 11794.

[1]B. D. Josephson, Adv. Phys. 14, 419 (1965).
[2]A. J. Dahm, A. Denenstein, T. F. Finnegan, D. N. Langenberg, and D. J. Scalapino, Phys. Rev. Lett. 20, 859 (1968).
[3]N. F. Pedersen, T. F. Finnegan, and D. N. Langenberg, Phys. Rev. B 6, 4151 (1972).
[4]A. Hoffman, Rev. Phys. Appl. 9, 312 (1974); Ph.D. thesis (Technischen Universitat Berlin, 1973) (unpublished).
[5]R. I. Gayley and T. C. Wang, Bull. Am. Phys. Soc. 20, 616 (1975).
[6]E. N. Economou, Phys. Rev. 182, 539 (1969).
[7]K. L. Ngai, Phys. Rev. 182, 555 (1969).
[8]P. B. Miller, Phys. Rev. 118, 928 (1960).
[9]D. D. Coon and M. D. Fiske, Phys. Rev. 138, A744 (1965).
[10] J. C. Swihart, J. Appl. Phys. 32, 461 (1961).
[11]I. O. Kulik, Zh. Tekh. Fiz. 37, 157 (1967) [Sov. Phys.-Tech. Phys. 12, 111 (1967)].
[12]K. Schwidtal and C. F. Smiley, in *Proceedings of the Thirteenth International Conference on Low Temperature Physics,* edited by K. D. Timmerhaus, W. J. O'Sullivan, and E. F. Hammel (Plenum, New York, 1974), Vol. 4, p. 575.
[13]Y. S. Gou and R. I. Gayley, Phys. Rev. B 10, 4584 (1974).
[14]O. H. Soerensen, T. F. Finnegan, and N. F. Pedersen, Appl. Phys. Lett. 22, 129 (1973).
[15]T. F. Finnegan, J. Wilson, and J. Toots, Rev. Phys. Appl 9, 199 (1974).
[16]D. N. Langenberg, D. J. Scalapino, and B. N. Taylor, Proc. IEEE 54, 560 (1966).
[17]A. B. Pippard, Proc. R. Soc. A 191, 385 (1947).
[18]E. H. Sondheimer, Adv. Phys. 1, 1 (1952).
[19]J. R. Waldram, Adv. Phys. 13, 1 (1964).
[20]S. Paley, J. Wilson, and R. I. Gayley, Phys. Lett. A 41, 311 (1972); Phys. Rev. B 12, 157 (1975).
[21]A typographical error in Ref. 13 caused this condition to appear as $(l\pi n\lambda_J)^2 \ll 1$.
[22]E. W. Economou (private communication).
[23]M. A. Biondi and M. P. Garfunkel, Phys. Rev. Lett. 2, 143 (1959); Phys. Rev. 116, 853 (1959).
[24]A. B. Pippard, Proc. R. Soc. A 203, 195 (1950); 203, 98 (1950).
[25]M. D. Sturge, Proc. R. Soc. A 246, 570 (1958).
[26]J. Matisoo, J. Appl. Phys. 40, 2091 (1969).